Journal of Physiology (1991), **437**, *pp.* 1–25
With 12 *figures*
Printed in Great Britain

INHIBITION OF CAUDAL MEDULLARY EXPIRATORY NEURONES BY RETROFACIAL INSPIRATORY NEURONES IN THE CAT

BY K. ANDERS*, D. BALLANTYNE†, A. M. BISCHOFF*, P. M. LALLEY‡§ AND D. W. RICHTER*

*From the † Physiologisches Institut, Universität Heidelberg, Im Neuenheimer Feld 326, D-6900 Heidelberg, Germany, the * Physiologisches Institut, Universität Göttingen, Humboldtallee 23, D-3400 Göttingen, Germany and the ‡ Department of Physiology, University of Wisconsin Medical Sciences Center, Service Memorial Institutes, 470 North Charter Street, Madison, WI 53706, USA*

(*Received 5 March 1990*)

SUMMARY

1. Comparisons between the spike discharge of inspiratory neurones within the retrofacial area (RFN), and the membrane potential of expiratory neurones within the caudal medulla were made in pentobarbitone-anaesthetized, vagotomized, artificially ventilated cats. Spike-triggered averaging (STA) of synaptic potentials, triggered by the discharge of inspiratory RFN neurones, was utilized to test for synaptic connectivity.

2. Eighty-nine neurones with respiratory-phased discharge patterns were recorded in the vicinity of the RFN. Fifty-four neurones discharged at or slightly before the onset of the inspiratory burst activity of the phrenic nerve and continued firing throughout inspiration. Two continued to fire during post-inspiration. Forty-five of fifty-four inspiratory RFN neurones exhibited incrementing discharge patterns, six discharged with a plateau pattern, while only three neurones had a decrementing discharge pattern.

3. The membrane potential trajectories of caudal expiratory neurones revealed a typical wave of early inspiratory hyperpolarization. Occasionally, a second wave of hyperpolarization occurred during late inspiration, in conjunction with increased phrenic nerve activity.

4. Spike-triggered averaging revealed averaged inhibitory postsynaptic potentials (IPSPs), indicative of inhibitory synaptic connections, between eight of sixty-three pairs of RFN inspiratory and caudal expiratory neurones.

5. Inhibitory postsynaptic potentials detected by STA exhibited a relatively long latency and a slow time course. The IPSPs began, on average, 3·8 ms after an RFN action potential. The rise times, half-widths and durations of IPSPs were longer than expected for a monosynaptic somal input from myelinated axons of inspiratory RFN

* Present address: Physiologisches Institut, Universität Göttingen, D-3400 Göttingen, Germany.

§ To whom correspondence and reprint requests should be addressed.

MS 7492

neurones. It is suggested that an inhibitory relay neurone in the immediate vicinity of the expiratory neurones is activated by a collateral of the RFN inspiratory neurone.

6. Retrofacial inspiratory neurones were antidromically activated only when high-intensity electrical stimulation was applied in the vicinity of caudal expiratory neurones.

7. The averaged IPSPs were preceded by diphasic and triphasic 'spike potentials'. The averaged spike potentials were highly entrained to the action potentials of RFN inspiratory neurones which triggered IPSPs. The spike potentials may be terminal potentials recorded from axons of RFN inspiratory neurones.

8. Evidence for convergence of synaptic inputs was obtained from STA tests in a caudal expiratory neurone receiving IPSPs from four RFN neurones.

9. The functional significance of this observation is discussed. We conclude that RFN inspiratory neurones exert a moderate inhibitory influence and act conjointly with other types of medullary inspiratory neurones.

INTRODUCTION

A population of expiratory neurones is located in the caudal medulla, from the level of the obex and lateral reticular nucleus, to the first cervical rootlets (Haber, Kohn, Ngai, Holoday & Wang, 1957; Merrill, 1974). Most of these neurones are bulbospinal with axon projections to the thoracic and upper lumbar levels of the spinal cord, where they provide a rhythmic, excitatory synaptic drive to expiratory motoneurones via a combination of monosynaptic and oligosynaptic pathways (Kirkwood & Sears, 1973; Cohen, Feldman & Sommer, 1985; Merrill & Lipski, 1987). Characteristically, expiratory neurones of the caudal medulla exhibit an augmenting pattern of discharge in deeply anaesthetized, vagotomized and artificially ventilated cats (Merrill, 1974). Intrinsic membrane conductance mechanisms may contribute in a number of ways to determine the pattern (Champagnat, Jacquin & Richter, 1986), but the incrementing character of the discharge results primarily from the action of synaptic inputs, the effect of which is to generate a ramp-like depolarization of the membrane on each cycle. Discharge is terminated at the transition from expiration to inspiration by a rapid membrane hyperpolarization which in many of these neurones gradually declines in amplitude as inspiration progresses; this is the result of an initially intense, but subsequently declining wave of chloride-dependent (inspiratory) inhibitory postsynaptic potentials (IPSPs). The transition from inspiration to expiration is followed by a similarly decrementing wave of (post-inspiratory) IPSPs containing both chloride-dependent and chloride-independent components, the effect of which is to delay the onset of expiratory discharge (D. Ballantyne and D. W. Richter, in preparation). In the simplest situation then, the membrane potential pattern of expiratory neurones is marked by the appearance of two IPSP waves of similar pattern and time course, one following the onset of inspiration and the other during post-inspiration. There is, however, an additional feature of the inhibitory control of these neurones which is much less well understood: in some recordings, the IPSP activity associated with the later stage of inspiration may be of an incrementing rather than decrementing character. Further, IPSP activity may not cease abruptly at the transition to expiration, but instead

persist at a low level well into the expiratory interval. In these neurones the typical wave of post-inspiratory IPSPs may emerge following a change in the overall pattern of respiration.

The origin of the various synaptic inputs responsible for the rhythmic activity of caudal expiratory neurones has not yet been established. The ramp-like development of expiratory depolarization might result from a rhythmic excitatory drive originating in expiratory neurones of the rostral medulla – a neuronal group commonly referred to as the 'Bötzinger complex' – in the vicinity of the retrofacial nucleus (RFN; Merrill, 1974; Fedorko & Merrill, 1984). It could, however, also result from a tonic excitatory drive (Bainton & Kirkwood, 1979) patterned by the decrementing wave of post-inspiratory IPSPs; in this case, the rhythmic nature of expiratory discharge would be attributable essentially to the rhythmic activation of those inhibitory neurones generating inspiratory and post-inspiratory IPSPs.

Sources for the inhibition might include early-burst inspiratory neurones of the nucleus retroambigualis (NRA), which send axon collaterals to the caudal, expiratory region of NRA (Merrill, 1974) and post-inspiratory neurones of NRA, whose discharge pattern and timing are consistent with the pattern of post-inspiratory inhibition (Richter, 1982; Richter & Ballantyne, 1983). A third possible source of synaptic inhibition is the population of inspiratory neurones in the RFN, in close proximity to the expiratory neurones of the Bötzinger complex. Various discharge patterns (early and late inspiratory, post-inspiratory) have been recorded within this area (Bianchi, Grélot, Iscoe & Remmers, 1988). RFN inspiratory neurones have been shown by antidromic mapping to project both to the contralateral NRA (Bianchi & Barillot, 1982) and RFN (Ezure & Manabe, 1988), and to inhibit expiratory neurones of the contralateral Bötzinger expiratory neurones (Ezure & Manabe, 1986). The object of the present study was to determine whether RFN inspiratory neurones represent a source of inhibition for expiratory neurones of the NRA. An abstract of the present study has been published (Lalley, Anders, Ballantyne, Bischoff & Richter, 1988).

METHODS

Results reported here were obtained from thirteen cats of either sex (2·5–4·5 kg), anaesthetized with sodium pentobarbitone, 35–40 mg kg^{-1} I.P. (initial dose), followed by supplementary I.V. doses of 4–8 mg as required. Supplementary doses were administered if elevations in blood pressure occurred during surgical preparation, or if during recording the normally stable pattern of phrenic nerve activity changed or blood pressure increased. Intravenous doses of gallamine triethiodide (4 mg kg^{-1} h^{-1}) were administered to achieve paralysis. Animals were artificially ventilated with oxygen-enriched room air. Ventilatory volume and rate were adjusted to maintain end-tidal CO_2 at 3–5 vol.%. Cannulas were placed in one femoral artery and both femoral veins, for monitoring blood pressure and for drug delivery, respectively. A cannula was inserted into the trachea below the larynx. The cat's head was mounted rigidly in a head holder and the spinous processes of T1 and L5 were clamped to a spinal frame. The head was ventroflexed for optimal exposure, after craniotomy, of the dorsal surface of the medulla. Phrenic (C5 branches) and cervical vagus nerves were exposed bilaterally through a dorsal approach, and were sectioned. Pneumothorax was established bilaterally to prevent respiratory movements and aid stability of recordings. Atelectasis was prevented by applying 1–2 cmH_2O of end-expiratory pressure to the expiratory outflow. Body temperature was maintained between 36 and 38 °C by external heating devices. The spinal cord was exposed by laminectomy from C2 and C4. Occipital craniotomy and retraction of the cerebellum exposed the obex and the region of the medulla overlying the RFN and the caudal NRA. Arachnoid and pial membranes were removed over the sites of microelectrode insertion. A

pressure foot was placed gently on the surface of the medulla, over the caudal NRA, to stabilize the brain tissue and increase stability of intracellular recording from caudal expiratory neurones.

An array of four bipolar concentric stainless-steel electrodes with tip diameters of 100 μm were inserted into the ventrolateral region of the spinal cord at C2–C3 in order to stimulate reticulospinal tracts and identify bulbospinal expiratory neurones by antidromic excitation and collision of action potentials. After electrode placement the spinal cord was covered with agar dissolved in Ringer solution. Cervical vagus nerves and desheathed phrenic nerves were mounted on bipolar silver hook electrodes for stimulation and recording, respectively. Phrenic nerve activity was amplified (2000–10000 ×), bandpass filtered (80–10000 Hz), displayed on an oscilloscope and registered on magnetic tape and chart-recorder (TA 2000, Gould, USA). Intracellular recordings were obtained from caudal expiratory neurones from obex level to approximately 2 mm caudal to the obex, located 2·5–3·0 mm lateral to the mid-line. Most recordings were made with micropipettes filled with 2 M-potassium citrate, however, a few cells were recorded with 3 M-KCl-filled micropipettes. DC resistances of microelectrodes in brain tissue ranged from 30 to 70 MΩ. Membrane potentials were recorded with a DC electrometer equipped with bridge balance and capacity compensation circuits, amplified (10 ×) and displayed on an oscilloscope. In most experiments, stainless-steel microelectrodes with tip resistances ranging from 5 to 12 MΩ, and in a few experiments glass microelectrodes filled with 4 M-NaCl (5–10 MΩ) were used to record extracellular activity of RFN neurones. Extracellularly recorded discharges of RFN inspiratory neurones were amplified (1000–2000 ×), bandpass filtered (30–3000 Hz) and displayed on an oscilloscope, and were also led off to a window discriminator which provided an output of uniform square pulses for presentation on a strip chart-recorder (TA 2000, Gould, USA), or for analog-to-digital conversion by a rate-meter. The rate-meter output was registered on strip chart paper as a moving average of discharge frequency (0·2 s time constant). Phrenic nerve activity was recorded on the chart-recorder, which also provided permanent records of membrane potential from expiratory neurones, arterial blood pressure and tracheal pressure.

Synaptic connectivity between RFN inspiratory and contralateral expiratory neurones was examined by the method of spike-triggered averaging (STA). STA was performed off-line from data recorded on magnetic tape. The action potentials of single RFN inspiratory neurones were converted to uniform square pulses and were used to trigger a programmable microprocessor-based signal averager. Averages of synaptic noise from caudal expiratory neurones were obtained with a microprocessor which digitized the analog input at a rate of 25 kHz. Synaptic noise presented to the microprocessor was amplified (2000–10000 ×) after filtering (0·1 Hz–10 kHz, or 1·0 Hz–10 kHz); in a few instances averages were also obtained with a bandwidth of DC–10 kHz in order to determine if filtering altered the shape of synaptic potentials or antecedent 'spike' potentials. It was clear from this type of analysis that filtering produced no changes in the shapes or amplitudes of averaged potentials. The majority of expiratory neurones tested exhibited maximal membrane potentials of −50 to −75 mV. In three neurones, membrane potential ranged from −35 to −45 mV. Normally, there was no overlap between the occurrence of action potentials in RFN inspiratory and caudal expiratory neurones, therefore it was unnecessary to attempt spike inactivation or suppression of discharge of caudal expiratory neurones with hyperpolarizing current. In the few instances where overlap occurred, a software program was used which rejected all samples preceding or following an action potential in the expiratory neurone by less than 50 ms. Averages were accepted only if there was no appreciable DC drift or large fluctuations of the amplified membrane potential during the sampling interval, and when at least 1500 consecutive samples could be obtained. Samples were averaged at sweep durations of 10 or 20 ms, and some re-averaged to include pre-trigger times of 3, 5 or 7 ms (sweep durations of 30 or 35 ms), in order to establish a baseline from the activity preceding the trigger.

Values of IPSP time course and amplitude were obtained by first establishing a baseline derived from the averaged noise level which preceded the trigger spike and IPSP. The onset latency and 10–90 % rise time of the IPSP were obtained from the point of intersection of the projected baseline and an extrapolated curve through the rising phase of the IPSP. Peak amplitude and duration of IPSPs were measured using the projected baseline as a reference.

To determine if the averaged synaptic potentials were entrained to the occurrence of an RFN inspiratory action potential, and not to external sources, averages were also obtained using an independent trigger source (waveform generator), in conjunction with the software program which excluded samples during expiration. The pulse frequency of the waveform generator was adjusted

to match the average discharge frequency of action potentials of the RFN neurone under inspection. Averaged potentials derived from RFN spike triggers were rejected if they exhibited periodicities similar to those triggered by the waveform generator, or if they did not exceed the averaged noise triggered by the waveform generator by at least a factor of three.

Segments of synaptic activity were also re-averaged, using phrenic nerve activity as the trigger, and pre-trigger times of 5, 7 or 10 ms, to test for the presence of high-frequency oscillations of potential (Cohen, 1973; Mitchell & Herbert, 1974; Kirkwood, Sears, Tuck & Westgaard, 1982; Ballantyne, Jordan, Spyer & Wood, 1988). Interspike interval histograms and autocorrelograms which revealed interspike intervals up to 100 ms were computed from RFN spike trains. Histograms and autocorrelograms were derived from the same samples of RFN action potentials which triggered averaged synaptic potentials in caudal expiratory neurones. The majority of histograms had no counts at zero time, and in those instances where they occurred, averages were rejected if more than 10% of the counts in the histogram were present at zero time, since this was taken as evidence for an appreciable contamination of averages by action potentials of more than one trigger neurone (Cohen & Feldman, 1984).

In six experiments attempts were made to antidromically activate inspiratory RFN neurones by stimulation within the pool of contralateral expiratory neurones. Clusters of expiratory neurones were first located by extracellular recording with metal microelectrodes (5–12 MΩ). In five experiments the same microelectrode was subsequently used for stimulation. Single pulses (50–200 μA, 0·05 ms duration) obtained from a constant-current stimulator were delivered through the microelectrode in the vicinity of expiratory neurones. In another experiment the microelectrode was withdrawn after locating caudal expiratory neurones and replaced by a concentric coaxial electrode for stimulation (inner pole diameter, 100 μm; outer diameter, 250 μm; DC resistance, 50 kΩ).

Recording sites in the RFN were marked by passing 0·1 μA of cathodal DC current for 10 min through glass microelectrodes to produce detectable lesions, or by passing cathodal current through metal microelectrodes in order to deposit iron at the tips. After the animal was killed with a lethal dose of sodium pentobarbitone, Ringer solution was perfused retrocardially, followed by 3% potassium ferrocyanide (w/v) to produce a Prussian Blue reaction product at sites of iron deposition. Fixation was produced by perfusion with 10% formaldehyde in Ringer solution (w/v). Frozen sections were mounted on slides and stained with Cresyl Violet for identification of recording sites. Sites where inspiratory neurones were recorded in the RFN were identified by the presence of the Prussian Blue reaction product, or by lesion and gliosis produced by current applied through glass microelectrodes.

RESULTS

The main result

From a population of fifty-four RFN respiratory neurones and seventy-five caudal expiratory neurones, sixty-three pairs were tested for connectivity. Neurones were selected solely on the basis of the quality and stability of the recording conditions. In the case of expiratory neurones, selection was based on the uniformity of membrane potential properties during STA, and on the absence of large membrane potential fluctuations which were not associated with the respiratory rhythm. RFN neurones were chosen for STA if they maintained an inspiratory pattern of discharge and if the spike discharge of individual neurones could be discriminated by the window detector when more than one neurone was recorded by the microelectrode.

Of the sixty-three pairs of inspiratory and expiratory neurones, thirty-seven pairs showed no evidence from STA of synaptic connectivity. Of the remaining twenty-six pairs which were further analysed because of the occurrence of averaged hyperpolarizing waveforms, four were subsequently disregarded due to multiunit recording when autocorrelograms and interval histograms revealed significant contamination by two or more neurones within the spike train from which positive

averages were obtained. Fourteen pairs showed evidence of a common input and/or high-frequency oscillations. The remaining eight pairs produced hyperpolarizing waves which were more than threefold larger in amplitude than baseline noise and gave no indication that they were attributable to high-frequency oscillations or

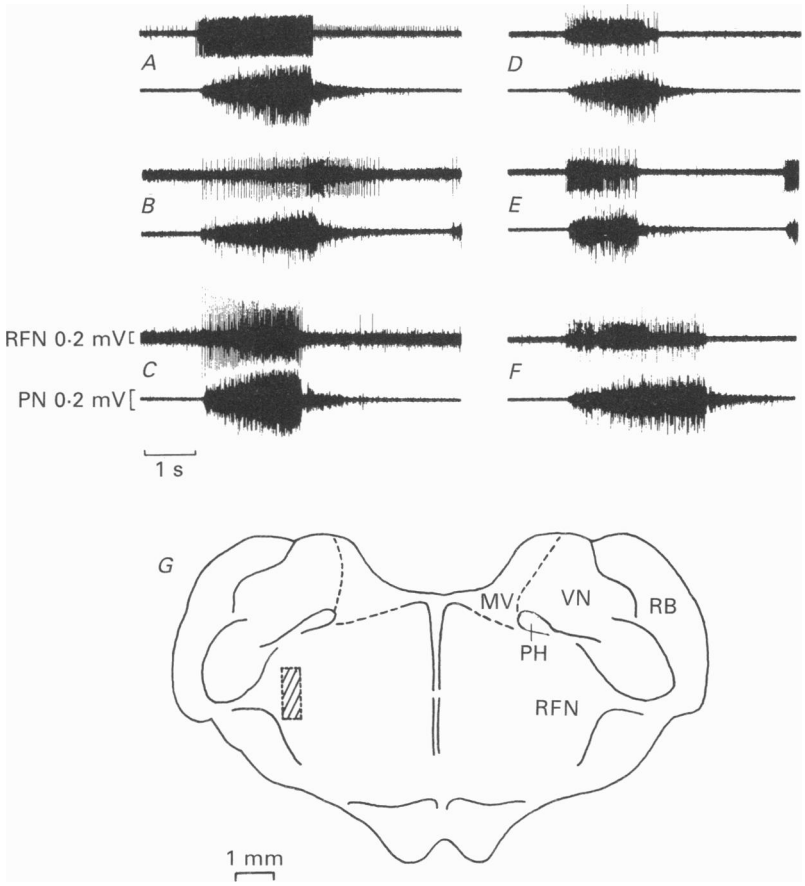

Fig. 1. Discharge patterns of RFN inspiratory neurones (upper traces *A–F*) in temporal relation to phrenic nerve discharges (PN). The location of fifteen of fifty-four RFN inspiratory neurones, identified histologically, is indicated by the hatched area in the scheme shown in *G*. MV, medial vestibular nucleus. PH, nucleus prepositus hypoglossi. VN, inferior vestibular nucleus. RB, restiform body. RFN, retrofacial nucleus.

common input. We assume that the waveforms recorded from these eight pairs represent IPSPs derived from inhibitory synaptic connections between RFN inspiratory neurones and caudal expiratory neurones.

Locations and discharge patterns of retrofacial respiratory neurones

Eighty-nine neurones which exhibited inspiratory- or expiratory-phased discharges were recorded extracellularly in the retrofacial region. Fifty-four revealed an inspiratory discharge, and thirty-five an expiratory discharge. They were found in

the vicinity of the RFN, 4–5 mm rostral to the obex, 3–3·5 mm lateral to the midline and 3·5–5·5 mm below the dorsal surface. This location is in agreement with the locations of RFN respiratory neurones reported by other laboratories (Lipski & Merrill, 1980; Bianchi & Barillot, 1982; Fedorko, Merrill & Lipski, 1983; Fedorko & Merrill, 1984).

Expiratory neurones were found in clusters at depths of 3·3–4·7 mm, immediately adjacent to a population of neurones which were presumed to be facial motoneurones, because they generated relatively large spikes in response to passive movement of the jaw or tactile stimulation. Inspiratory neurones were found in greatest numbers medial to the expiratory population at depths ranging from 3·3 to 4·7 mm. Neurones which discharged during late inspiration or post-inspiration were encountered relatively infrequently. They were located ventral to inspiratory and expiratory neurones at depths of 5–5·5 mm. The location of inspiratory neurones is shown in Fig. 1. This population includes neurones which were found by STA to have inhibitory synaptic connections with caudal expiratory neurones. Most inspiratory neurones (forty-five of fifty-four) exhibited an incrementing discharge pattern. Representative examples of their discharge patterns are illustrated, along with phrenic nerve activities, in Fig. 1 *A–F*.

The pattern of discharge exhibited by individual RFN inspiratory neurones was stable throughout the period of recording except in one instance where a burst-type acceleration of discharge sometimes occurred towards the end of inspiration (see Figs 1*B* and 3). Figure 1 *A–C*, top traces, show incrementing discharge patterns of three RFN inspiratory neurones which gave rise to STA-averaged IPSPs. The RFN neurone giving large spikes in *A* began firing just before the onset of phrenic nerve burst activity, showed an increase in frequency shortly thereafter and an abrupt termination at the end of inspiration (i.e. at the peak of the ramp-like phrenic nerve burst). The RFN neurone illustrated in *B* exhibits a gradual increase in firing frequency which reached a maximum at the end of the inspiration and a decline during the post-inspiratory after-discharge in the phrenic nerve. The discharge illustrated in Fig. 1*C* represents the firing of three RFN neurones, as revealed by inspection on the oscilloscope and from high-speed strip chart-recording (not shown). One neurone, producing the smallest spike in record *C*, fired infrequently during expiration, but the other two neurones in this record discharged only during inspiration, their activity beginning with the onset of inspiration and ceasing at the peak of inspiratory activity in the nerve. The large spike of one of these two neurones, the spike showing an incrementing pattern of activity, was used to trigger the averaged IPSPs shown in Figs 4 and 5. The discharge shown in Fig. 1*D* contains the spikes of three neurones. The neurone which discharged at the highest frequency began to fire with the onset of phrenic nerve activity and ceased firing at the peak of the latter. The action potentials of this particular neurone, but not the others, produced an averaged IPSP in an expiratory neurone. In Fig. 1*E* also, the discharge contained spikes from three RFN inspiratory neurones. The neurone giving rise to medium-sized action potentials discharged briskly with the onset of phrenic nerve activity, then slowed during the later part of inspiration. Action potentials from this neurone triggered hyperpolarizing waveforms, examples of which are shown in Fig. 10*A* and *B*, which further analysis suggested (see later) were derived from a synaptic

input common to both the RFN inspiratory and the caudal expiratory neurone. In Fig. 1*F* the neurone discharging medium-sized spikes exhibited a firing pattern which reached maximum frequency before the middle of the phrenic nerve burst. Averaged IPSPs were observed using action potentials of this RFN neurone as a

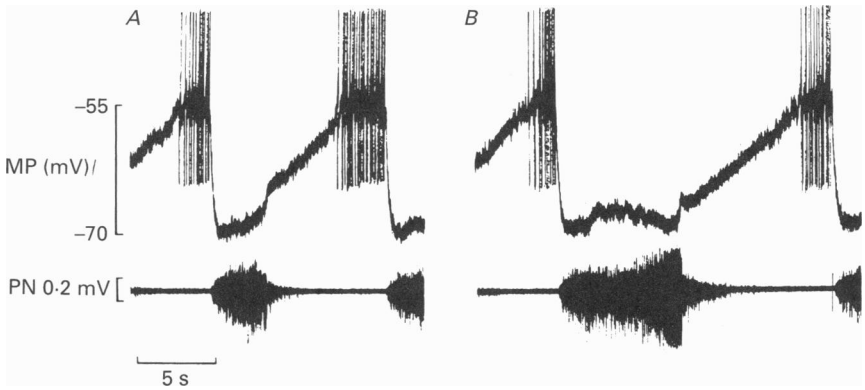

Fig. 2. Membrane potential (MP) and discharge patterns of a caudal expiratory neurone (*A* and *B*), together with phrenic nerve discharges (PN). A typical pattern with a relatively smooth, declining wave of hyperpolarization coinciding with the beginning of the ramp-like phrenic nerve discharge is illustrated in *A*. The recording of the same expiratory neurone shown in *B* displays a second wave of membrane hyperpolarization during late inspiration and membrane hyperpolarization during post-inspiration is slowed. Action potentials are truncated.

trigger source, whereas in the same expiratory neurone averages of the synaptic noise triggered by the larger spikes in *D*, *E* and *F* showed no evidence of a response.

Relatively few inspiratory RFN neurones ($n = 9$) were encountered which exhibited non-incrementing (plateau or decrementing) discharge patterns. Most could not be recorded long enough to test for synaptic connectivity. Six of these neurones displayed plateau patterns, i.e. discharges which began abruptly with inspiration, continued at a uniform rate and terminated abruptly at the end of inspiration. Three of the neurones exhibited a decrementing discharge during inspiration.

Membrane potential patterns of caudal expiratory neurones

The membrane potential patterns and discharge properties of caudal expiratory neurones have been previously described in detail (Mitchell & Herbert, 1974; Ballantyne & Richter, 1986). The typical behaviour of caudal expiratory neurones is shown by the example in Fig. 2*A* where the hyperpolarizing wave of IPSPs is largest at the beginning of inspiration and becomes smaller as inspiration progresses. In this example, as well as in all recordings obtained with microelectrodes containing potassium citrate, membrane hyperpolarization during inspiration reached transient peak levels and the synaptic noise remained visible throughout membrane hyperpolarization. This was taken to indicate that the membrane hyperpolarization was positive to the equilibrium potential of IPSPs.

Transient waves of membrane hyperpolarization were also recorded occasionally from caudal expiratory neurones accompanying spontaneous changes in phrenic nerve activity. An example is seen in Fig. 2*B*, where a second wave of hyperpolarization during late inspiration occurred in association with a late-

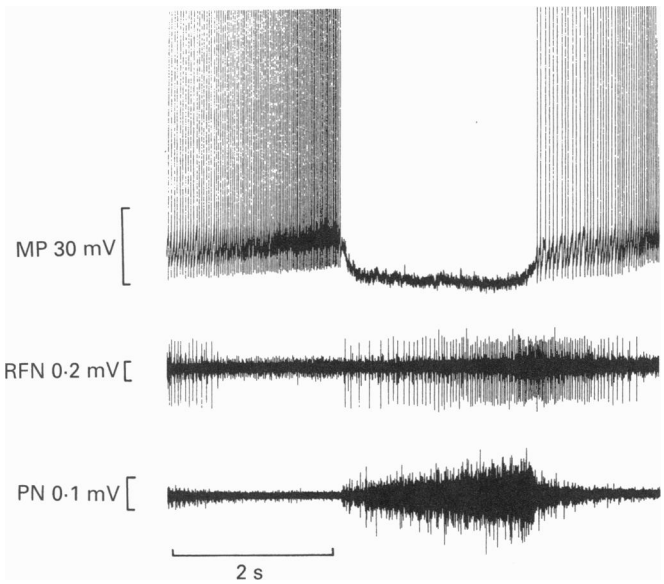

Fig. 3. Relationship of RFN inspiratory discharge to membrane potential (MP) of caudal expiratory neurone. The RFN neurone exhibited an incrementing discharge (middle trace) during inspiration and a waning discharge during post-inspiration (compare with phrenic nerve discharge, PN, bottom trace) and overlaps with the firing of the expiratory neurone (top trace).

inspiratory increase in phrenic burst discharge. Similar transient changes in the otherwise stable pattern of expiratory neurone and phrenic nerve activities have also been reported by Ballantyne & Richter (1986). A less pronounced wave of late-inspiratory hyperpolarization recorded from another expiratory neurone is shown in Fig. 3.

In this example a shallow, late-inspiratory hyperpolarization occurs in the presence of a smooth augmenting pattern of phrenic nerve activity. The middle trace of Fig. 3 illustrates the discharge of an RFN neurone which begins during inspiration and continues on into the post-inspiratory after-discharge in the phrenic nerve. The frequency of action potentials increased as the second wave of hyperpolarization of the expiratory neurone developed. Thereafter a transient burst of spikes at higher frequency occurred during the ramp-like depolarization. The RFN neurone continued to fire at gradually decreasing frequency following the transition to expiration when the membrane potential of the caudal expiratory neurone depolarized and the latter started to discharge action potentials at gradually increasing frequency.

There was no obvious relationship between the discharge patterns of inspiratory

RFN neurones and the pattern of inspiratory hyperpolarization of expiratory neurones.

In Fig. 4, for example, the membrane hyperpolarization of a spike-inactivated expiratory neurone decreased as the frequency of action potentials of the inspiratory

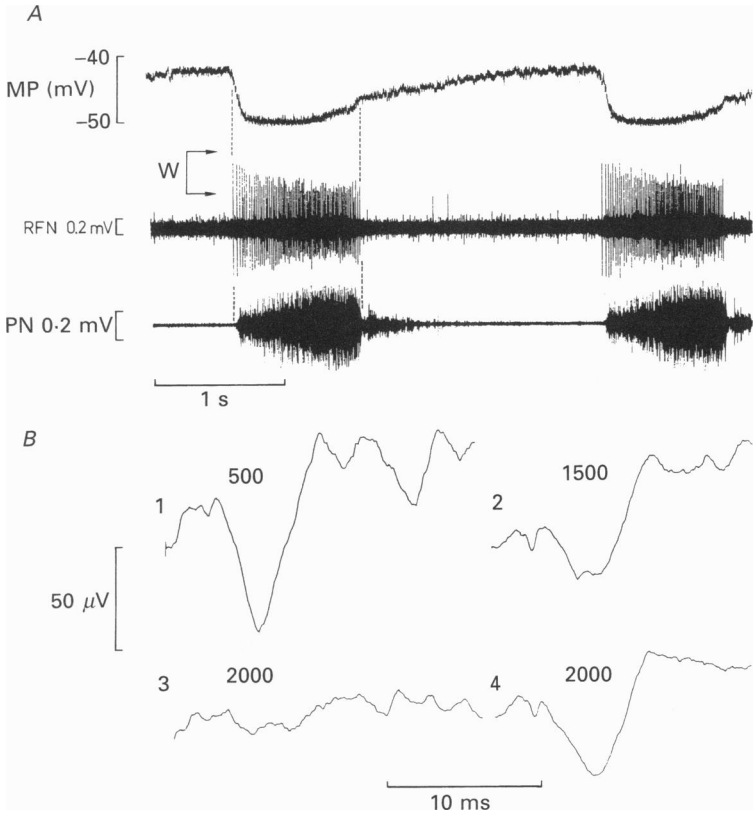

Fig. 4. IPSPs recorded from an inactivated caudal expiratory neurone (*A*, top trace). Action potentials of the RFN neurone with an incrementing discharge pattern (middle trace) were detected by a window discriminator (window width indicated by arrows and W). Action potentials triggered the acquisition of 20 ms segments of synaptic noise which were averaged to produce the IPSPs illustrated in *B*, traces 1, 2 and 4. *B*1 is the average of the first 500 segments, *B*2 includes the segments from *B*1 plus an additional 1000 samples, *B*4 includes the segments of *B*1 and *B*2 plus an additional 500 consecutive samples. *B*3 is the average of 2000 samples triggered by a waveform generator which produced random square pulses at the mean frequency of the RFN action potentials.

RFN neurone increased. This observation leads to the conclusion that RFN neurones are not the sole source of synaptic inhibition of caudal expiratory neurones, but presumably reinforce the action of other respiratory neurones in suppressing and delaying the onset of firing in caudal expiratory neurones.

Investigation of synaptic connectivity using spike-triggered averaging

Spike potentials

Averages obtained from twenty-two of fifty-nine pairs selected for analysis (Methods) showed a hyperpolarizing potential of long time course (Table 1) following the trigger. In each of these twenty-two averages the trigger was also followed by a

TABLE 1. Properties of averaged IPSPs and 'spike potentials' ($n = 8$)

	Mean	Range
IPSPs:		
Onset latency (ms)	3·8	1·9–6·1
Time to peak (ms)	4·3	2·1–6·4
Rise time, 10–90 % (ms)	2·7	1·2–4·8
Half-width (ms)	6·5	3·2–8·2
Duration (ms)	12·2	6·1–15·9
Amplitude (μV)	16·0	3·0–32·0
'Spike potentials':		
Onset latency (ms)	2·3	1·9–2·9
Width (ms)	0·5	0·47–0·53
Amplitude (μV)	23·0	5·0–89·0

biphasic or triphasic potential of short time course; in any given case the latency of this potential was virtually constant in successive averages (Figs 6*E* and 8*E*). It was absent from all thirty-six averages for which there was no evidence of an accompanying hyperpolarizing response. Measurements of the spike potentials were made in eight averages where the properties of averaged synaptic potentials were judged to be IPSPs (see below). For the eight averages the width of the spike potentials, measured from onset to termination, ranged from 0·47 to 0·53 ms. Two of the averaged spikes were of relatively large amplitude (57 and 89 μV) whereas those remaining ranged in size from 5 to 39 μV (average, 9 μV). In six of eight cases, the spike potentials preceded the averaged IPSPs by 0·9–3·7 ms (average, 1·5 ms). In two cases it was not possible to reliably distinguish between the point at which the spike potential occurred and the slower, hyperpolarizing potential began. The onset of the IPSP must have occurred in the interval between the beginning and the end of the spike potential (spike widths, 0·5 and 0·53 ms). For the eight averages, the interval from trigger spike to spike potential ranged from 1·9 to 2·9 ms (mean interval, 2·3 ms).

Synaptic potentials giving evidence of inhibitory connections

Averages from eight pairs of neurones exhibited hyperpolarizing waves which were more than threefold larger in amplitude than baseline noise, had a sharp 'take-off' from baseline and for each average showed little variability in the interval between the trigger spike and the onset of hyperpolarization. These waveforms gave no indication that they were attributable to high- or medium-frequency oscillations or to common synaptic input (see below). We assume that these waveforms represent

IPSPs and reflect the activation of an inhibitory pathway between RFN inspiratory and caudal expiratory neurones.

On average, the IPSPs recorded from the eight pairs began 3·8 ms after the trigger spikes of an RFN inspiratory neurone, and reached a peak 4·3 ms after the onset of

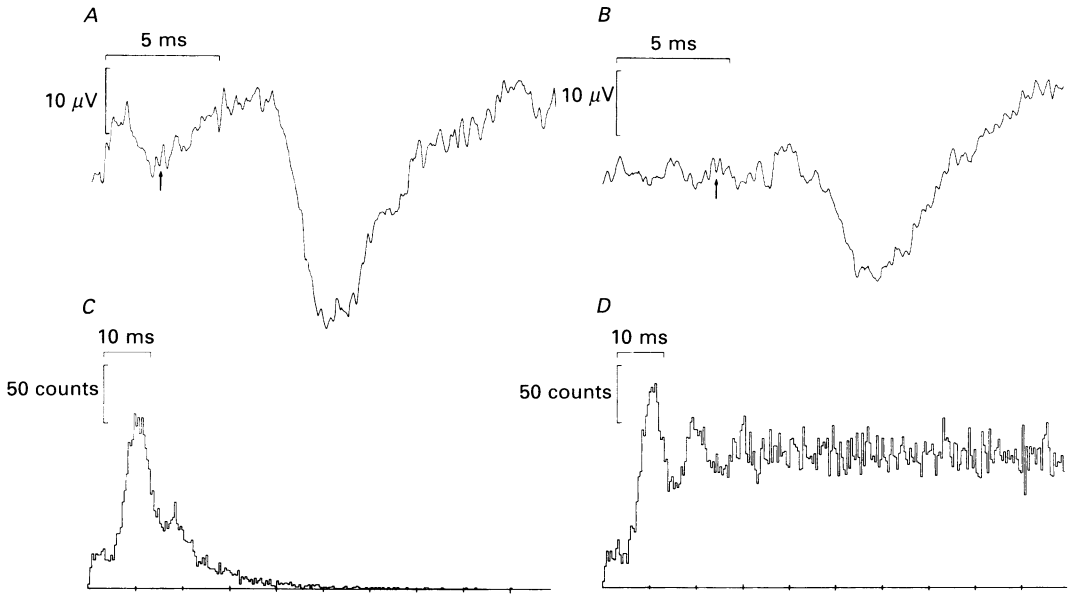

Fig. 5. Averaged IPSPs and properties of RFN spike trains. *A* and *B*, averaged IPSPs from the same caudal expiratory neurone shown in Fig. 4. *C*, interval histogram of RFN inspiratory spike train from which IPSPs were triggered. *D*, autocorrelogram of RFN inspiratory spike train. In *A*, 3 ms of averaged synaptic noise precedes the RFN trigger spikes. In *B*, 5 ms of averaged synaptic noise precedes the trigger spike. Occurrences of the trigger spikes are denoted by arrows.

the IPSP. Average mean rise time (10–90 %), half-width and peak amplitude were 2·7 ms, 6·5 ms and 16 μV, respectively. Two of the expiratory neurones from which the averaged IPSPs were recorded were also tested for spinal projections by stimulating the spinal cord at C3. Both neurones were activated antidromically. The properties of averaged IPSPs derived from these two expiratory neurones did not differ significantly from those detected in neurones which were not tested for antidromic activation.

Examples of averaged IPSPs are shown along with the discharge properties of the pairs of neurones from which they were obtained in Figs 4, 7 and 9. Statistical properties of spike trains along with the corresponding averaged IPSPs are illustrated in Figs 5, 6 and 8.

Averaged IPSPs from one pair are illustrated in Figs 4 and 5. In Fig. 4 the RFN inspiratory neurone which triggered the averaging of IPSPs was isolated by window discrimination, as shown in the middle trace (window denoted by W). Values for time

course and amplitude were obtained from records such as those shown in Fig. 5. The values for the IPSPs were: onset latency, 5·1 ms; latency from onset to peak, 2·2 ms; duration, 6·1 ms; rise time, 1·2 ms; half-width, 3·2 ms; amplitude, 17 μV. The interval histogram and autocorrelogram (Fig. 5*C* and *D*) show a preferred interval of approximately 10 ms.

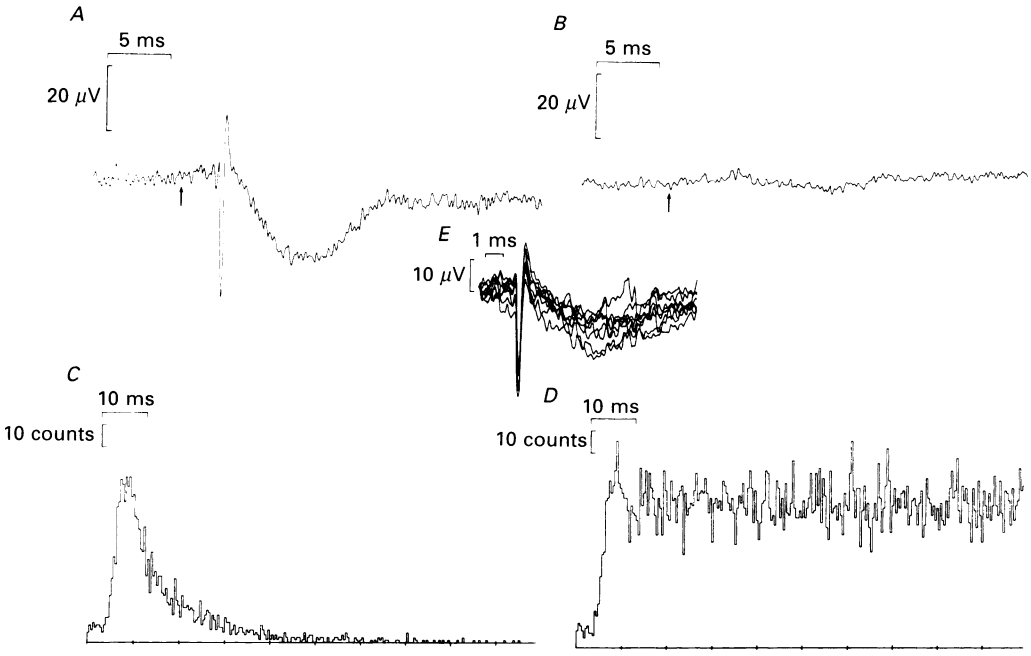

Fig. 6. Averaged IPSP recorded from a caudal expiratory neurone (also illustrated in Fig. 9*B*, trace 3), and properties of the spike train recorded from an RFN inspiratory neurone (I_3). *A*, averaged IPSP derived from 2000 samples. Pre-trigger time, 7 ms. Arrow denotes occurrence of RFN inspiratory trigger spikes. *B*, average of 2000 samples, 7 ms pre-trigger time, triggered by pulses from a waveform generator. Arrow denotes trigger pulses. *C*, interval histogram of spike train recorded from RFN inspiratory neurone, I_3. *D*, autocorrelogram of I_3 spike train. *E*, superimposition of eight averages, each average derived from 500 sweeps.

Figure 6 shows another example of an averaged hyperpolarizing response. Records 6*A* and *E* show averaged IPSPs. The trigger spike (occurrence denoted by the arrow) is preceded in *A* by 7 ms of synaptic noise. The IPSP begins 4·2 ms after the trigger spike of the RFN inspiratory neurone and reaches a peak 5·4 ms after onset. Values for rise time, half-width and amplitude are 3·3 ms, 7·7 ms and 23 μV, respectively. The IPSP is preceded, by 1·3 ms, by a large spike potential. Record *B* shows an essentially flat average derived from an independent trigger source (waveform generator). As shown in records *C* and *D* the RFN neurone which triggered the averaged IPSP shown had a preferred interspike interval of 8·9 ms.

Examples of reversed postsynaptic potentials (PSPs) that were recorded in one

experiment with a KCl-filled microelectrode are illustrated in Figs 7 and 8. The IPSPs underwent rapid reversal to depolarizing PSPs without a need for ejecting additional chloride with negative current. Averaged depolarizing PSPs were observed after spontaneous waves of membrane hyperpolarization during inspiration had converted

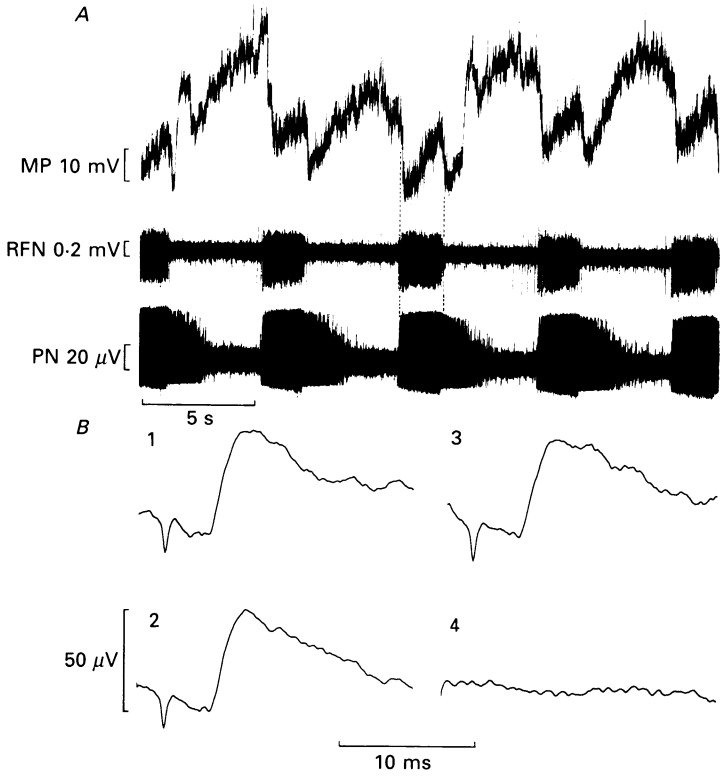

Fig. 7. Depolarizing PSPs recorded from a caudal expiratory neurone with a KCl-filled microelectrode. Top trace in *A* shows incrementing waves of depolarizing IPSPs following leakage of chloride ions from the microelectrode. The inspiratory waves of PSPs coincide with the discharges of the inspiratory RFN neurone, as indicated by the vertical dashed lines. Averages of depolarizing PSPs in *B* were generated by 5000 (*B*1 and 2) and 10000 (*B*3) action potentials of the inspiratory RFN neurone (*A*, middle trace). *B*4 illustrates the averaged potential triggered by the waveform generator.

to depolarizing waves. We, therefore, assume that the nature of the PSP is inhibitory and chloride dependent.

The upper trace in Fig. 7*A* illustrates waves of depolarizing PSPs in the expiratory neurone, which coincide with incrementing discharges of an RFN inspiratory neurone and with inspiratory firing recorded from the phrenic nerve. The reversal of IPSPs is quite evident although the pattern differs from the more typical declining type of inspiratory inhibition described in detail by Ballantyne & Richter (1986). Various averages of the depolarizing PSPs are illustrated also in Fig. 8, along with

the statistical properties of the spike train recorded from the RFN neurone. The averaged IPSPs had a sharp onset (Fig. 8*A* and *B*) after a constant latency (Fig. 8*E*).

The reversed PSP began 6·1 ms after the trigger spike and reached a peak at 2·1 ms after onset. Values for rise time, half-width and amplitude are 1·3 ms, 6·1 ms and

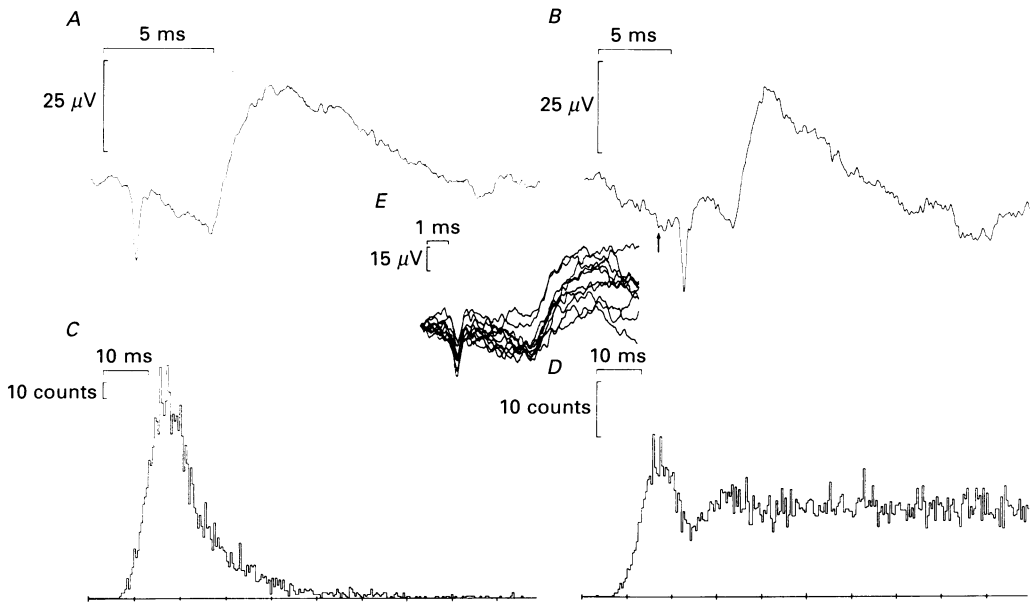

Fig. 8. Depolarizing PSPs recorded from the caudal expiratory neurone shown in Fig. 7, and properties of the RFN inspiratory spike trains. *A* and *B*, averaged PSPs from the expiratory neurone. *A*, average of 5000 samples. Start of average coincides with the occurrence of RFN inspiratory trigger spikes. *B*, average of 5000 samples, 5 ms pre-trigger time. Arrow denotes time of trigger spikes. *C*, interval histogram of RFN inspiratory spike train. *D*, autocorrelogram of spike train. *E*, superimposition of ten averages. Each average is derived from 1000 sweeps.

32 μV, respectively. Figure 8*C* and *D* indicate that the averaged PSPs were derived from spikes of a single RFN neurone which discharged at a preferred interval of 15 ms.

Convergence and divergence of RFN projections

From one experiment, it was possible to detect convergence and divergence of inhibition originating from RFN inspiratory neurones. Results are illustrated in Fig. 9. IPSPs triggered by an RFN neurone were detected in two different caudal expiratory neurones, one of which exhibited IPSPs associated with the discharges of four of seven RFN inspiratory neurones tested. Part *A* of Fig. 9 is a schematic illustration of synaptic connectivity. An RFN inspiratory neurone (I_4) is shown from STA to be connected to two contralateral expiratory neurones (E_1 and E_2). The caudal expiratory neurone E_1 receives inhibitory synaptic input from RFN neurones I_1–I_4, as evidenced by the averaged IPSPs shown in part *B*, where trace 1 is the IPSP

triggered by RFN neurone I_1, trace 2 was triggered by I_2, etc. Part *C* displays the discharge patterns of neurones I_1–I_4 as standardized pulses derived from the Schmitt trigger output of a window discriminator. Part *D* shows two consecutive bursts of phrenic nerve activity in the upper trace, and intracellular records from caudal

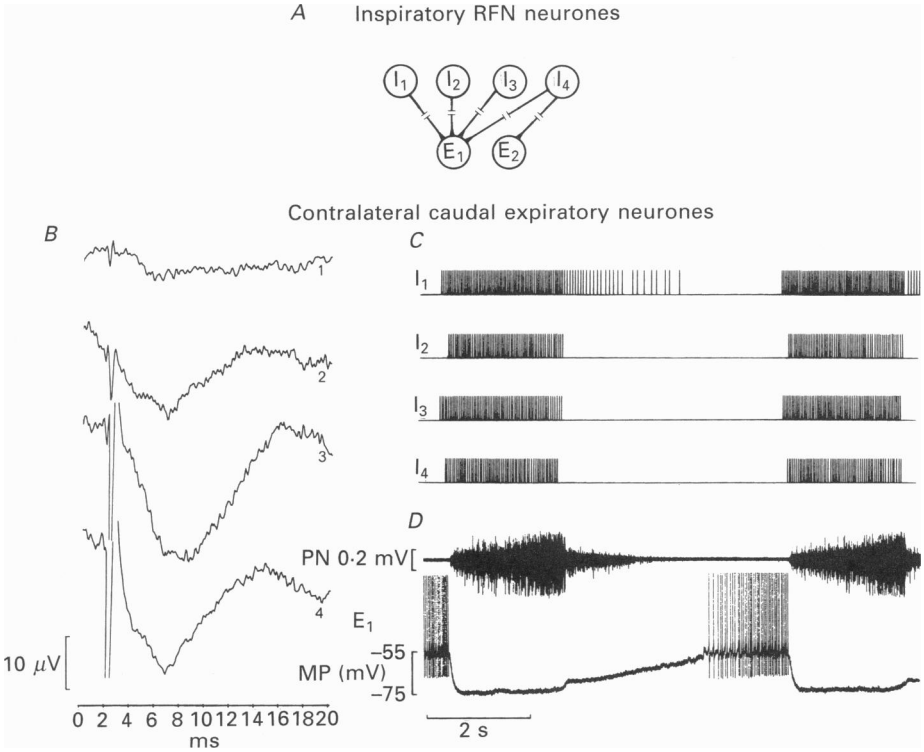

Fig. 9. Connectivity between RFN inspiratory and caudal expiratory neurones, illustrating convergence and divergence. *A* is a schematic illustration of synaptic connectivity. Four inspiratory RFN neurones converge on the caudal expiratory neurone E_1. Divergence is seen by the projection of RFN neurone I_4 to caudal expiratory neurones E_1 and E_2. The traces 1–4 shown in *B* are averaged IPSPs recorded from the expiratory neurone E_1 during the discharges of the inspiratory neurones I_1–I_4. *C* illustrates the normalized spike discharge of the RFN neurones I_1–I_4. *D* shows phrenic nerve activity (PN) and the membrane potential (MP) of the expiratory neurone E_1. See text for further description.

expiratory neurone E_1 in the lower trace. There was some variation in the interburst intervals of RFN, phrenic nerve and caudal expiratory neurone discharges during the various STA tests. Therefore, each of the traces in *C* was selected from a large sample of RFN bursts, recorded simultaneously with E_2 and phrenic nerve activity during STA, to match the temporal pattern of phrenic nerve activity shown in part *D*. This was done in order to illustrate the discharge pattern and to relate the discharges of all four RFN neurones to a single pattern of phrenic nerve activity. The four RFN neurones fired throughout inspiration, and one of the neurones (I_1) continued to discharge at a lower frequency during post-inspiration. The IPSPs

triggered by RFN neurones I_1–I_4 in caudal expiratory neurone E_2 varied in amplitude, shape and time course, and as in other experiments, it was not possible to relate these parameters to the discharge patterns of any RFN neurone. One of the IPSPs shown in Fig. 9*B* (trace 3) is shown in greater detail in Fig. 6.

Evidence for synchronization of inputs

Averages from six pairs of neurones revealed evidence suggesting that the discharge of a number of RFN inspiratory neurones might be synchronized to each other. We assume, by analogy with cross-correlograms computed by other laboratories from pairs of extracellularly recorded spike trains, that the averages reflect synchronization between RFN neurones, or an input shared by the RFN and caudal expiratory neurones (Kirkwood & Sears, 1980; Feldman & Speck, 1983). Several of these inputs, including the one providing the trigger, could inhibit caudal expiratory neurones. Figure 10, traces *A* and *B*, gives examples of averages which were considered as evidence for a common synaptic input. The average in *A* was obtained without a pre-trigger interval, and gives the appearance of an essentially flat baseline preceding a spike potential and the wave of hyperpolarization. However, the average with a pre-trigger time of 5 ms (*B*) shows that a wave of depolarization precedes the wave of hyperpolarization. The depolarizing wave precedes the RFN trigger spike by 1·9 ms, whereas the onset of the wave of hyperpolarization follows by 4·2 ms. This waveform does not appear to be associated with high- or medium-frequency oscillations, since the autocorrelograms of phrenic nerve activity and the firing of the RFN trigger neurone showed no evidence for a periodicity. The averaged waveform might arise from some type of shared synaptic input. The waveform appears to differ in shape, however, from those which represent common presynaptic input to intercostal motoneurones (Kirkwood & Sears, 1978). One additional average exhibited waves of depolarization preceding and following the averaged hyperpolarizing waveform. In this case, it was not possible to determine with certainty the onset, time course and amplitude of the wave of hyperpolarization.

High- and medium-frequency oscillations

Averages obtained from seven pairs (pre-trigger times of 5 or 7 ms) revealed membrane potential oscillations of 47–80 Hz. Similar oscillations were sometimes detected when phrenic nerve activity was used as a trigger source. Figure 10, traces *C* and *D*, illustrates examples of oscillatory waves (47 Hz) recorded from a caudal expiratory neurone. In *C*, the beginning of the waveform (average of 1000 sweeps) is coincident with the occurrence of trigger spikes from an RFN inspiratory neurone. Tracing *D* is the averaged waveform (500 sweeps), shown on a slower time scale, with a pre-trigger time of 10 ms. The arrow in *D* denotes the occurrence of the trigger spikes. Synchronous waves were also observed in averages when phrenic nerve activity was used as the trigger source. It is assumed that these waveforms are high-frequency oscillations in expiratory neurones, which have also been observed by other laboratories (Mitchell & Herbert, 1974; Ballantyne, Jordan, Spyer & Wood, 1988).

Antidromic tests

Antidromic mapping experiments of Bianchi & Barillot (1982) showed that axons of RFN inspiratory neurones are found nearby in the ventral respiratory group. We therefore determined whether RFN inspiratory neurones could be antidromically

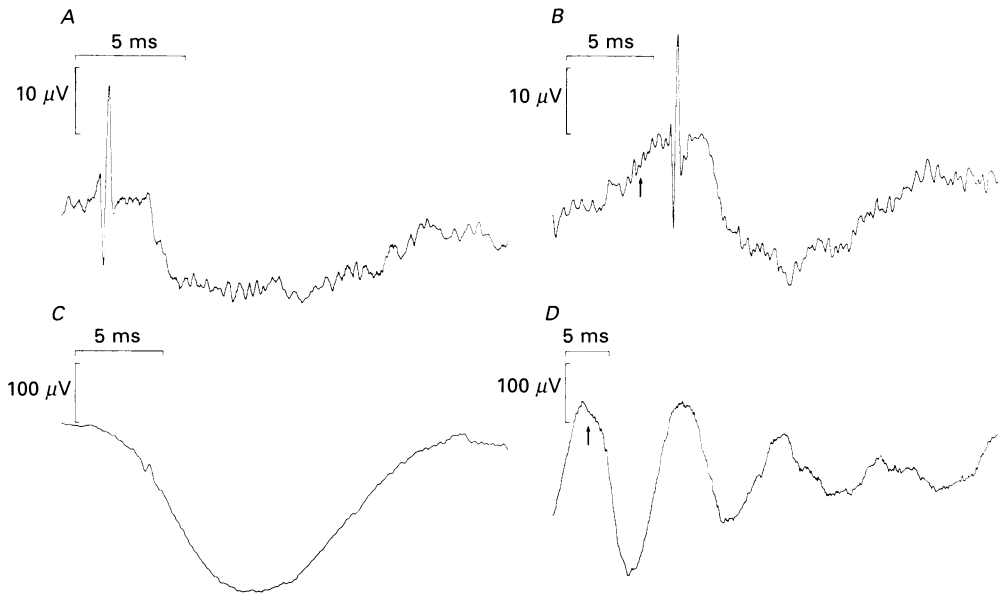

Fig. 10. Examples of averages obtained from two expiratory neurones (*A* and *B* from one neurone; *C* and *D* from another) which suggest common synaptic input or high-frequency oscillations. *A* and *B*, averages which suggest occurrence of common input to RFN and caudal expiratory neurone. *A*, start of average coincides with the occurrence of RFN trigger spikes. Average derived from 5000 samples. *B*, average of 5000 samples with a pre-trigger time of 5 ms. Arrow denotes occurrence of RFN trigger spikes. Note occurrence of depolarizing wave which begins before the trigger spikes of the RFN inspiratory neurone. *C* and *D*, averages which suggest occurrence of high-frequency oscillations. *C*, averages of 1000 samples. Start of the average coincides with the occurrence of trigger spikes. *D*, average of 500 samples. Note different time scale. Onset of the average precedes the trigger spike (arrow). Waveform exhibits 47 Hz oscillation.

activated by stimulation within the pool of caudal expiratory neurones. In these experiments, clusters of expiratory neurones were first located by extracellular recordings with metal microelectrodes (5–12 MΩ). In five experiments the same microelectrode was subsequently used for stimulation. Single pulses (50–200 μA, 0·05 ms duration) derived from a constant-current stimulator, however, failed to elicit antidromic responses of RFN neurones. Extensive mapping within the area was not performed. In one experiment, stimuli delivered through a concentric bipolar electrode resulted in antidromic activation of seven of eight RFN inspiratory neurones, as revealed by collision testing. Thresholds for antidromic activation of the seven RFN inspiratory neurones ranged from 0·8 to 2·0 mA. Latencies for antidromic

activation ranged from 1·97 to 4·60 ms (mean latency 3·39 ms). Antidromic activation of one RFN neurone is illustrated in Fig. 11. Part *A* of Fig. 11 shows the discharge pattern of an RFN neurone. Firing begins with the onset of phrenic nerve activity and persists throughout inspiration. Part *B* shows the results of collision tests on this

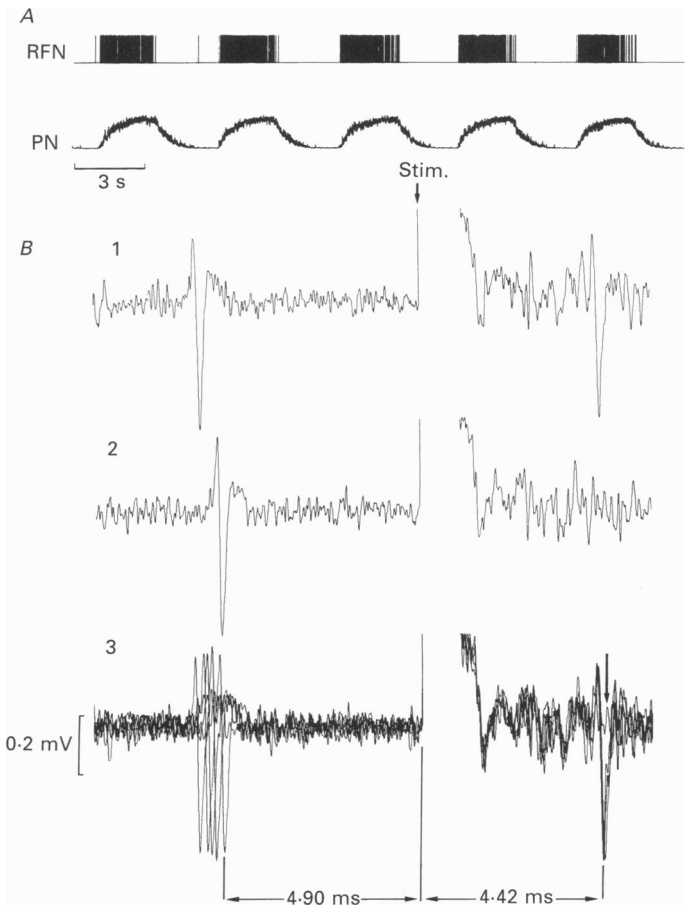

Fig. 11. Antidromic activation of an inspiratory RFN neurone, evoked by stimulation within the pool of caudal expiratory neurones. *A*, inspiratory RFN neurone discharge pattern (RFN), and integrated phrenic nerve activity (PN). *B*, traces 1–3, test for collision. *B*1, electrical stimulation (Stim) evokes an antidromic action potential in the RFN neurone after a latency of 4·42 ms. Note that the spontaneous action potential (left) precedes the stimulus by an interval longer than 4·90 ms. *B*2, failure of antidromic excitation, indicating collision, when the interval between the spontaneous action potential and the stimulus is 4·90 ms. *B*3, superimposition of five traces. Four of the five stimuli evoked an antidromic potential. Collision occurred when a spontaneous action potential preceded the stimulus by 4·90 ms. The stimulus required for antidromic activation was a 2 mA, 50 μs square pulse.

neurone and demonstrates that the neurone is activated antidromically. Traces 1–3 indicate that the antidromic latency was 4·42 ms and the critical delay was greater than 4·90 ms. In *B*1, the interval between a spontaneous action potential and the

stimulus was greater than 4·9 ms, thus an antidromically evoked action potential is evident. A similar situation applies to four out of five tests shown in *B*3.

DISCUSSION

Of the various inputs which have been proposed to inhibit caudal expiratory neurones (Richter, Ballantyne & Remmers, 1986), RFN inspiratory neurones were chosen for investigation in the present experiment. The selection was made on the basis of findings from other laboratories which indicated that inspiratory RFN neurones project axons near to a region within the contralateral medulla where inspiratory and expiratory neurones are located (Bianchi & Barillot, 1982). The results of cross-correlation analysis (Hilaire, Monteau & Bianchi, 1984) suggest that inspiratory neurones of the NRA are synaptically activated by inspiratory RFN neurones. Comparable studies of the connectivity between RFN inspiratory and NRA expiratory neurones have not been reported. This investigation reveals that RFN inspiratory neurones provide a source of inhibition to expiratory neurones. The relatively long latencies involved and the slow time course of this inhibition raise a number of questions as to the nature of the underlying connection and these are considered in turn below.

The first possibility to be considered is that they reflect an inhibitory synaptic connection between RFN inspiratory neurones and caudal expiratory neurones. Averaged IPSPs of eight pairs reveal only a small degree of variability in latency and exhibit a sharp take-off. This steep take-off became especially clear in a reversed depolarizing IPSP. We assume, therefore, that the IPSPs are directly related to the discharge of the inspiratory RFN trigger spike. On the assumption that the IPSPs recorded from these eight pairs are indeed linked to the action potential discharge of RFN neurones, the next question to be considered is whether the inhibition occurs over a mono- or disynaptic pathway connecting RFN inspiratory and caudal medullary expiratory neurones. Concerning this question, factors which must be considered are: (1) source of the spike potential, (2) latencies, (3) shape indices of the averaged IPSPs.

Spike potentials

Spike-like changes in potential ('spike potentials') became evident in all averages derived from a single trigger spike in which membrane hyperpolarizations were observed ($n = 22$). The spike potentials were tightly entrained to the RFN trigger spike, suggesting that they are derived from the axons of the latter. The considerably large amplitudes of seventeen spike potentials and the diphasic configuration could indicate terminal field potentials of axons (Meyers & Snow, 1986; Dick, Vanna & Berger, 1988). We propose that a relatively large percentage of the RFN neurones have axons which terminate in the vicinity of caudal expiratory neurones. The IPSPs, which exhibit shape indices indicative of a disynaptic event, are then mediated by a collateral of the RFN inspiratory neurone which terminates at an interposed relay neurone, located in the immediate vicinity of the expiratory neurone. Kreuter *et al.* identified neighbouring expiratory and inspiratory neurones

at the level of the obex (Kreuter, Richter, Camerer & Senekowitsch, 1977), where some of the hyperpolarizing waves were recorded in this study. An inspiratory-phased interneurone might exhibit a non-stationary discharge pattern which would reduce the likelihood that the terminal potential is detected in averages triggered by an RFN neurone.

Latencies of terminal spike potentials and IPSPs

The latency to the spike potentials ranged from 1·9 to 2·9 ms (mean, 2·3 ms). If the spike potentials were produced over a monosynaptic pathway, then the conduction velocity of the RFN axons could be estimated by the distance between retrofacial and medullary regions. In such a calculation we took into account that axons of respiratory neurones in the RFN region cross the mid-line at the level of their origin before descending caudally, as suggested by anatomical studies (Otake, Sasake, Manneu & Ezure, 1987) and shown electrophysiologically (Bianchi & Barillot, 1982). From this information we determined a conduction distance of 13 mm between the RFN and caudal expiratory neurones and calculated a conduction velocity of the axon of 4·4–6·7 m s^{-1}. This range of velocity spans the mean value of 6·1 m s^{-1} of inspiratory RFN neurones obtained in antidromic mapping experiments by Bianchi & Barillot (1982).

Six of the eight averaged IPSPs began 3·1–6·1 ms after the trigger spike. We could not measure precisely the latency of two averaged IPSPs, since the terminal spike potential masked their onset. However, the error of measurement would not have exceeded 0·5 ms, which represents the width of the terminal spike. An error of $\pm$0·5 ms does not change the mean value of 3·8 ms for the eight values. There is, on average, a 1·5 ms delay between the occurrence of the terminal potentials and the onset of the IPSPs, which allows the possibility that a relay neurone is activated and synaptically inhibits the caudal expiratory neurone.

Shape indices

The values for latency (3·8 ms), rise time (2·7 ms), half-width (6·6 ms) and duration (12·2 ms) found in the present investigation are greater than those known for monosynaptic IPSPs detected by STA in a variety of neurones such as neck motoneurones (Rapoport, Susswein, Uchino & Wilson, 1977), hindlimb motoneurones (Jankowska & Roberts, 1972), phrenic motoneurones (Merrill & Fedorko, 1984) and inspiratory neurones of the nucleus tractus solitarii (NTS; Merrill, Lipski, Kubin & Fedorko, 1983). In the latter study, IPSPs recorded in inspiratory neurones, and triggered by expiratory RFN ('Bötzinger') neurones, had latencies of 1·6–2·0 ms, half-width times of 1·6–3·5 ms, and 10–90% rise times of 0·45–0·86 ms. The IPSPs in phrenic motoneurones related to the firing of Bötzinger expiratory neurones revealed the following parameters: half-width, 1·6–3·2 ms; rise time 0·5–1·4 ms (Merrill & Fedorko, 1984). The slow time course of the averaged IPSPs recorded in the present investigation might, therefore, be related to one or more of several possibilities. First, the IPSPs could be generated by inspiratory interneurones synaptically activated by RFN inspiratory neurones. Thus, the averaged IPSPs would be associated with a disynaptic pathway. Comparison with averaged IPSPs in other neurones favours such an explanation. Lumbar motoneurones reveal IPSPs

after activation of the Ia disynaptic pathway (Watt, Stauffer, Taylor, Reinking & Stuart, 1976), and also via interneurones driven by medullary reticulospinal neurones (Takakusaki, Ohta & Mori, 1989). The rise times of these disynaptic IPSPs were 0·6–2·7 ms, and 1·79 ± 0·84 ms (means ± S.D.), respectively. In the present study the mean rise time was 2·7 ms (range, 1·2–4·8 ms), which is indicative of a disynaptic pathway. However, a second possibility that must be considered is that the connections are monosynaptic, the IPSPs originating in synapses at relatively remote locations on dendrites of expiratory neurones and electrotonic spread is responsible for slowing the voltage changes produced by the synapse.

Other sorts of RFN spike-triggered hyperpolarizations

Inspiratory and expiratory neurones may exhibit rapid oscillations (50–120 Hz) of membrane potential during inspiration and these involve chloride-dependent conductance changes (Mitchell & Herbert, 1974; Ballantyne, Jordan, Spyer & Wood, 1988). In the present study we have identified such synchronization in seven pairs of neurones. Synchronization became evident when the trigger neurone and the membrane potential of the expiratory neurone showed evidence of periodicity in the range of 50–120 Hz. Synchronization of RFN inspiratory neurones might also have contributed to the slow time course of some averaged hyperpolarizing waves. Presynaptic synchronization could also account for the occurrence of some IPSPs which exhibited average waveforms exemplified by Fig. 10 *B*.

Antidromic testing

Our tests for antridromic activation were restricted in the sense that stimulation was applied only to the regions where clusters of expiratory neurones were recorded. No attempt was made to localize discrete axonal projections inside or outside of this region. Only when stimulation was applied through a large electrode was it possible to evoke antidromic firing of RFN inspiratory neurones. The large current intensities might have caused current spread for some distance outside the location of expiratory neurones. Bianchi & Barillot (1982) evoked antidromic responses from inspiratory RFN neurones by monopolar stimulation, 0·5–1·5 mm rostral to the obex,with microelectrodes using intensities of 5–50 μA (0·1 ms pulse duration). In the present experiments stimulating electrodes were positioned 0·5–1·5 mm caudal to the obex. Our failure to locally activate axons of inspiratory RFN neurones by microstimulation may be explained by a diffuse distribution of small branches of RFN axons within the caudal NRA.

Contribution of RFN inspiratory neurones to the inhibition of caudal expiratory neurones

It seems clear from these results that inspiratory neurones in the region of RFN contribute to the synaptic inhibition of caudal expiratory neurones. Averaged IPSPs were triggered by RFN neurones which discharged at the beginning and throughout the inspiratory phase and also during post-inspiration. We suggest that inspiratory RFN neurones, which discharge throughout the inspiratory phase, act conjointly with early inspiratory neurones (Richter, 1982) to produce inhibition of caudal expiratory neurones.

In Fig. 12, a schematic illustration summarizes the relative contribution of various synaptic inputs to the membrane potential behaviour of the caudal expiratory neurone. The integrated phrenic nerve discharge (top) is shown along with the time–insensity profile of the membrane potential of a caudal expiratory neurone

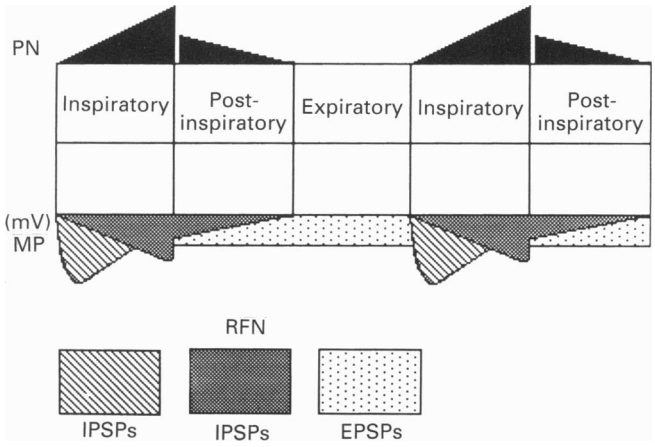

Fig. 12. Schematic summary of synaptic inputs controlling the membrane potential properties of a caudal expiratory neurone. The membrane potential trajectories resulting from convergence of inhibitory (▨ and ■) and excitatory (⊡) afferents to caudal expiratory neurones are schematically illustrated. The finding of inhibitory connections between inspiratory RFN neurones and caudal expiratory neurones would explain late-inspiratory and post-inspiratory inhibition (■).

(bottom). The scheme highlights the following points: (1) there is a tonic input of excitatory postsynaptic potentials (EPSPs) which ultimately produces an expiratory-phased discharge of action potentials; (2) EPSPs are shunted by IPSPs during inspiration and post-inspiration. There is evidence (Richter, 1982) that the declining wave of inspiratory IPSPs (■) originates from early-inspiratory propriobulbar neurones whereas a declining wave of post-inspiratory inhibition is attributed to a different class of post-inspiratory neurones. IPSPs produced by RFN inspiratory neurones are also depicted. It is assumed that IPSPs in caudal expiratory neurones occur predominantly during the inspiratory period and some also during post-inspiration. The pattern associated with a given RFN inspiratory neurone remains stable during normal, quiet breathing, and the consequent synaptic inhibition of caudal expiratory neurones is assumed to be relatively moderate. The functional significance of the waves of IPSPs set up by RFN inspiratory neurones may be to reinforce the declining inhibition of early inspiratory neurones (Richter, Ballantyne & Remmers, 1987), so to control the onset of post-inspiration and guarantee a normal sequence of the respiratory cycle.

The authors wish to thank Frau A. Kühner for technical assistance. We also thank Dr Richard Moss, Department of Physiology, University of Wisconsin and Dr Steve Mifflin, Department of Pharmacology, University of Texas, San Antonio for reading and criticizing a draft of this manuscript. P.M.L. was the recipient of a Fogarty Senior International Fellowship (National Institutes of Health), a Guest Professor Stipendium (University of Heidelberg) and a

research/study grant from Deutscher Akademischer Austrauschdienst. Research supported by the Deutsche Forschungsgemeindschaft, United States Public Health Service grant HL29563, and by funds from a United States Public Health Service General Research Support grant to the University of Wisconsin Medical School.

REFERENCES

BAINTON, C. R. & KIRKWOOD, P. A. (1979). The effect of carbon dioxide on the tonic and rhythmic discharges of expiratory bulbospinal neurones. *Journal of Physiology* **296**, 291–314.

BALLANTYNE, D., JORDAN, D., SPYER, K. M. & WOOD, L. M. (1988). Synaptic rhythm of caudal expiratory neurones during stimulation of the hypothalamic defence area of the cat. *Journal of Physiology* **405**, 527–546.

BALLANTYNE, D. & RICHTER, D. W. (1986). The non-uniform character of expiratory synaptic activity in expiratory bulbospinal neurones of the cat. *Journal of Physiology* **370**, 433–456.

BIANCHI, A. L. & BARILLOT, J. C. (1982). Respiratory neurons in the region of the retrofacial nucleus: pontile, medullary, spinal and vagal projections. *Neuroscience Letters* **31**, 277–282.

BIANCHI, A. L., GRÉLOT, L., ISCOE, S. & REMMERS, J. E. (1988). Electrophysiological properties of rostral medullary respiratory neurones in the cat: an intracellular study. *Journal of Physiology* **407**, 293–310.

CHAMPAGNAT, J., JACQUIN, T. & RICHTER, D. W. (1986). Voltage-dependent currents in neurones of the nuclei of the solitary tract of rat brainstem slices. *Pflügers Archiv* **406**, 372–379.

COHEN, M. I. (1973). Synchronization of discharge, spontaneous and evoked, between inspiratory neurons. *Acta Neurobiologica Experimentalis* **33**, 189–218.

COHEN, M. I. & FELDMAN, J. L. (1984). Discharge properties of dorsal medullary inspiratory neurons: Relation to pulmonary afferent and phrenic efferent discharges. *Journal of Neurophysiology* **51**, 753–776.

COHEN, M. I., FELDMAN, J. L. & SOMMER, D. (1985). Caudal medullary expiratory neurone and internal intercostal discharges in the cat: effects of lung inflation. *Journal of Physiology* **368**, 147–178.

DICK, T. E., VANNA, F. & BERGER, A. J. (1988). Electrophysiological determination of the axonal projections of single dorsal respiratory group neurones to the cervical spinal cord of the cat. *Brain Research* **454**, 31–39.

EZURE, K. & MANABE, M. (1986). An origin of inspiratory inhibition of expiratory neurons in the Bötzinger complex. *Journal of the Physiological Society of Japan* **48**, 384.

EZURE, K. & MANABE, M. (1988). Decrementing expiratory neurones of the Bötzinger complex. *Experimental Brain Research* **27**, 159–166.

FEDORKO, L. & MERRILL, E. G. (1984). Axonal projections from the rostral expiratory neurones of the Bötzinger complex to medulla and spinal cord in the cat. *Journal of Physiology* **350**, 487–496.

FEDORKO, L., MERRILL, E. G. & LIPSKI, J. (1983). Two descending medullary inspiratory pathways to phrenic motoneurones. *Neuroscience Letters* **43**, 285–291.

FELDMAN, J. L. & SPECK, D. F. (1983). Interactions among inspiratory neurons in the dorsal and ventral respiratory groups in cat medulla. *Journal of Neurophysiology* **49**, 472–490.

HABER, E., KOHN, K. W., NGAI, S. H., HOLODAY, D. A. & WANG, S. C. (1957). Localization of spontaneous respiratory neuronal activities in the medulla oblongata of the cat: a new location of the expiratory center. *American Journal of Physiology* **190**, 350–355.

HILAIRE, G., MONTEAU, R. & BIANCHI, A. L. (1984). A cross-correlation study of interactions among respiratory neurons of dorsal, ventral and retrofacial groups in cat medulla. *Brain Research* **302**, 19–31.

JANKOWSKA, E. & ROBERTS, W. J. (1972). Synaptic actions of single interneurones. *Journal of Physiology* **222**, 623–642.

KIRKWOOD, P. A. & SEARS, T. A. (1973). Monosynaptic excitation of thoracic motoneurones from lateral respiratory neurones in the medulla of the cat. *Journal of Physiology* **234**, 87–89*P*.

KIRKWOOD, P. A. & SEARS, T. A. (1978). The synaptic connexions to intercostal motoneurones as revealed by the average common excitation potential. *Journal of Physiology* **275**, 103–134.

KIRKWOOD, P. A. & SEARS, T. A. (1980). The measurement of synaptic connections in the central nervous system by means of spike-triggered averaging. In *Progress in Clinical Neurophysiology*, vol. 8, ed. DESMEDT, J. E., pp. 44–71. Karger, Basel.

KIRKWOOD, P. A., SEARS, T. A., TUCK, D. L. & WESTGAARD, R. H. (1982). Variations in the time course of the synchronization of intercostal motoneurones in the cat. *Journal of Physiology* **327**, 105–135.

KREUTER, F., RICHTER, D. W., CAMERER, H. & SENEKOWITSCH, R. (1977). Morphological and electrical description of medullary respiratory neurons of the cat. *Pflügers Archiv* **372**, 7–16.

LALLEY, P. M., ANDERS, K., BALLANTYNE, D., BISCHOFF, A. M. & RICHTER, D. W. (1988). Inhibition of caudal expiratory neurones by retrofacial inspiratory neurones. *Neuroscience Abstracts* **14**, (1), 626.

LIPSKI, J. & MERRILL, E. G. (1980). Electrophysiological demonstration of the projection from expiratory neurones in rostral medulla to contralateral dorsal respiratory group. *Brain Research* **197**, 521–524.

MERRILL, E. G. (1974). Finding a respiratory function for the medullary respiratory neurone. In *Essays on the Nervous System*, ed. BELLAIRS, R. & GRAY, E. G., pp. 451–486. Clarendon, Oxford.

MERRILL, E. G. & FEDORKO, L. (1984). Monosynaptic inhibition of phrenic motoneurons: a long descending projection from Bötzinger neurons. *Journal of Neuroscience* **4**, 2350–2353.

MERRILL, E. G. & LIPSKI, J. (1987). Inputs to intercostal motoneurons from ventrolateral medullary respiratory neurons in the cat. *Journal of Neurophysiology* **57**, 1837–1853.

MERRILL, E. G., LIPSKI, J., KUBIN, L. & FEDORKO, L. (1983). Origin of the expiratory inhibition of nucleus tractus solitarius inspiratory neurones. *Brain Research* **263**, 43–50.

MEYERS, D. E. R. & SNOW, P. J. (1986). Distribution of activity in the spinal terminations of single hair follicle afferent fibers to somatotopically identified regions of the cat spinal cord. *Journal of Neurophysiology* **51**, 1022–1038.

MITCHELL, R. A. & HERBERT, D. A. (1974). The effect of carbon dioxide on the membrane potential of medullary respiratory neurones. *Brain Research* **75**, 345–349.

OTAKE, K., SASAKE, H., MANNEU, H. & EZURE, K. (1987). Morphology of expiratory neurons of the Bötzinger complex: An HRP study in the cat. *Journal of Comparative Neurology* **258**, 565–579.

RAPOPORT, S., SUSSWEIN, A., UCHINO, Y. & WILSON, V. J. (1977). Synaptic actions of individual vestibular neurones on cat neck motoneurones. *Journal of Physiology* **272**, 367–382.

RICHTER, D. W. (1982). Generation and maintenance of the respiratory rhythm. *Journal of Experimental Biology* **100**, 93–108.

RICHTER, D. W. & BALLANTYNE, D. (1983). A three phase theory about the basic respiratory pattern generator. In *General Neurone Environment and the Control Systems of Breathing and Circulation*, ed. SCHLAFKE, M. E., KOEPCHEN, H. P. & SEE, W. R., pp. 164–174. Springer Verlag, Berlin.

RICHTER, D. W., BALLANTYNE, D. & REMMERS, J. E. (1986). How is respiratory rhythm generated? A model. *News in Physiological Sciences* **1**, 109–112.

RICHTER, D. W., BALLANTYNE, D. & REMMERS, J. E. (1987). The differential organization of medullary postinspiratory activities. *Pflügers Archiv* **410**, 420–427.

TAKAKUSAKI, K., OHTA, Y. & MORI, S. (1989). Single medullary reticulospinal neurones exert postsynaptic inhibitory effects via inhibitory interneurons upon alpha-motoneurons innervating cat hindlimb muscles. *Experimental Brain Research* **74**, 11–23.

WATT, D. C. D., STAUFFER, E. K., TAYLOR, A., REINKING, R. M. & STUART, D. C. (1976). Analysis of muscle receptor connections by spike-triggered averaging. 1. Spindle primary and tendon organ afferents. *Journal of Neurophysiology* **39**, 1375–1392.